Redox Biology 70 (2024) 103080

Contents lists available at ScienceDirect

Redox Biology

journal homepage: www.elsevier.com/locate/redox

DDAH1 recruits peroxiredoxin 1 and sulfiredoxin 1 to preserve its activity and regulate intracellular redox homeostasis

Juntao Yuan [a,1], Zhuoran Yu [a,1], Ping Zhang [b,1], Kai Luo [a], Ying Xu [a], Ting Lan [a], Min Zhang [c,**], Yingjie Chen [d,***], Zhongbing Lu [a,*]

[a] College of Life Science, University of Chinese Academy of Sciences, Beijing, 100049, China
[b] Division of Hematology, Oncology and Transplantation, Department of Medicine, University of Minnesota, Minneapolis, 55455, USA
[c] Department of Nephrology, Affiliated Beijing Chaoyang Hospital of Capital Medical University, Beijing, 100020, China
[d] Department of Physiology & Biophysics, University of Mississippi Medical Center, Jackson, MS, 39216, USA

ARTICLE INFO

Keywords:
DDAH1
ADMA
Oxidative stress
PRDX1
SRXN1

ABSTRACT

Growing evidence suggests that dimethylarginine dimethylaminohydrolase 1 (DDAH1), a crucial enzyme for the degradation of asymmetric dimethylarginine (ADMA), is closely related to oxidative stress during the development of multiple diseases. However, the underlying mechanism by which DDAH1 regulates the intracellular redox state remains unclear. In the present study, DDAH1 was shown to interact with peroxiredoxin 1 (PRDX1) and sulfiredoxin 1 (SRXN1), and these interactions could be enhanced by oxidative stress. In HepG2 cells, H_2O_2-induced downregulation of DDAH1 and accumulation of ADMA were attenuated by overexpression of PRDX1 or SRXN1 but exacerbated by knockdown of PRDX1 or SRXN1. On the other hand, DDAH1 also maintained the expression of PRDX1 and SRXN1 in H_2O_2-treated cells. Furthermore, global knockout of *Ddah1* (*Ddah1*$^{-/-}$) or liver-specific knockout of *Ddah1* (*Ddah1*^{HKO}) exacerbated, while overexpression of DDAH1 alleviated liver dysfunction, hepatic oxidative stress and downregulation of PRDX1 and SRXN1 in CCl_4-treated mice. Overexpression of liver PRDX1 improved liver function, attenuated hepatic oxidative stress and DDAH1 downregulation, and diminished the differences between wild type and *Ddah1*$^{-/-}$ mice after CCl_4 treatment. Collectively, our results suggest that the regulatory effect of DDAH1 on cellular redox homeostasis under stress conditions is due, at least in part, to the interaction with PRDX1 and SRXN1.

1. Introduction

Oxidative stress, which is caused by the overproduction of reactive oxygen species (ROS) and the impairment of the antioxidant system, triggers various biochemical reactions such as lipid peroxidation, DNA damage, and protein oxidative modifications or misfolding [1,2]. Growing evidence suggests that oxidative stress plays an important role in the pathogenesis of numerous diseases, including nonalcoholic fatty liver disease (NAFLD) [3], diabetes [4], and cardiovascular disease [5]. Understanding the mechanism involved in the regulation of intracellular redox homeostasis is essential for the treatment of clinically relevant diseases.

Dimethylarginine dimethylaminohydrolase 1 (DDAH1) is recognized as a critical enzyme for the degradation of asymmetric dimethylarginine (ADMA) [6], which inhibits nitric oxide synthase (NOS) by competing with L-Arg. Our studies have consistently shown that DDAH1 can repress oxidative stress in different disease models, including fatty liver [7,8], muscle injury and regeneration [9], diabetic nephropathy [10] and $PM_{2.5}$-exposed lung [11]. As ADMA accumulation under pathological conditions can promote ROS production by uncoupling NOS [12] or upregulating the renin–angiotensin system [13], the antioxidant effect of DDAH1 may be partly attributed to ADMA degradation. We previously also demonstrated that the deletion of *Ddah1* in mouse embryonic fibroblasts (MEFs) increased intracellular ROS levels through a miR-21-dependent pathway [14], suggesting that DDAH1 may have an additional mechanism of regulation of the cellular redox state.

* Corresponding author. College of Life Science, University of Chinese Academy of Sciences, 19A Yuquanlu, Beijing, 100049, China.
** Corresponding author.
*** Corresponding author.
E-mail addresses: cyyyzm@139.com (M. Zhang), ychen2@umc.edu (Y. Chen), luzhongbing@ucas.ac.cn (Z. Lu).
[1] These three authors contribute equally to this work.

https://doi.org/10.1016/j.redox.2024.103080
Received 18 January 2024; Received in revised form 4 February 2024; Accepted 7 February 2024
Available online 8 February 2024
2213-2317/© 2024 The Authors. Published by Elsevier B.V. This is an open access article under the CC BY-NC-ND license (http://creativecommons.org/licenses/by-nc-nd/4.0/).

Additionally, DDAH1 contains several cysteine (Cys) residues and is sensitive to oxidative stress. DDAH1 activity or expression is reduced by hydrogen peroxide (H_2O_2) or homocysteine [15,16]. However, whether there is a potential mechanism to protect DDAH1 activity or expression under conditions of oxidative stress has not been investigated.

Peroxiredoxin 1 (PRDX1) is a representative antioxidant enzyme that scavenges H_2O_2 and alkyl hydroperoxide involved in redox signaling pathways. However, PRDX1 can be overoxidized by excess H_2O_2 under conditions of extreme oxidative stress, leading to enzyme inactivation. The reduction of overoxidized PRDX1 is catalyzed by sulfiredoxin 1 (SRXN1) [17]. In addition to sensing redox signaling, PRDX1 is involved in signal transduction through noncovalent protein−protein interaction [18]. As shown in the Biogrid interaction database [19], there are 338 unique PRDX1 interactors (accessed 10/31/2023). For example, PRDX1 interacts with mammalian Ste20-like kinase-1 (MST-1) and stimulates MST-1 autophosphorylation and activation [20]. PRDX1 also functions as a tumor repressor by inhibiting c-Myc-mediated transcription via protein interaction [21]. To fully understand the roles of PRDX1 in signal transduction and cellular function, it is necessary to further analyze the interacting partners of PRDX1 in different models.

In the present study, we found that PRDX1 and SRXN1 interacted with DDAH1 and maintained its expression and activity in HepG2 cells and the livers of carbon tetrachloride (CCl_4)-challenged mice. However, DDAH1 also attenuated PRDX1 downregulation and oxidation after oxidative stimulation.

2. Materials and methods

Detailed information on the experimental materials is listed in Table S1.

2.1. Mice and experimental Design

The generation and genetic backgrounds of *Ddah1*$^{-/-}$ mice and DDAH1 transgenic (DDAH1-TG) mice were described in our previous studies [11,22]. In brief, *Ddah1* gene was first deleted in the sperm through crossing the DDAH1$^{flox/flox}$ mice with the protamine (Prm)-Cre mice. The obtained male Prm-Cre/DDAH1$^{flox/+}$ mice were then crossed with wild-type (WT) female mice to obtain *Ddah1*$^{+/-}$ mice. The heterozygotes were crossed with WT C57BL/6J mice for more than 10 generations and then used to obtain the *Ddah1*$^{-/-}$ mice. The DDAH1-TG mice were generated by Cyagen Biosciences Inc. (Jiangsu, China) through microinjection a human DDAH1 transgenic vector into the pronuclei of fertilized one-cell mouse embryos of C57BL/6J mice. The vector contains an EF1A promoter, human DDAH1 coupled with 3xFLAG epitope on N-terminus, and RNA processing signals from SV40 polyA. Age-matched C57BL/6J mice were used as WT controls. Eight-week-old *Ddah1*$^{f/f;Alb-ERT2-cre/+}$ mice were injected intraperitoneally with tamoxifen (50 mg/kg/day) for 5 consecutive days to establish hepatocyte-specific *Ddah1* knockout mice (*Ddah1*^{HKO}) [7]. *Ddah1*$^{f/f}$ littermates were administered the same dose of tamoxifen and then used as controls. The mice were kept in temperature-controlled (22 ± 2 °C) SPF rooms under a 12:12 h light–dark cycle and fed distilled water and commercial mouse food *ad libitum*.

Eight-week-old male C57BL/6J, *Ddah1*$^{-/-}$, DDAH1-TG, *Ddah1*$^{f/f}$ and *Ddah1*^{HKO} mice were randomly divided into control and CCl_4 treated groups (8–10 mice/group). CCl_4 was dissolved in olive oil before injection. Mice were injected intraperitoneally with 1 g/kg CCl_4 or with olive oil every other day three times. At the end of the experiments, the mice were sacrificed via CO_2 inhalation followed by spinal cord dislocation, and blood and liver tissue collection for biochemical analyses.

The liver-specific promoter (thyroxine-binding globulin)-driven AAV8-*Prdx1* and AAV8-*GFP* expression vectors were produced by Vigene Biosciences Inc. (Shandong, China). Hepatic PRDX1 overexpression in WT and *Ddah1*$^{-/-}$ mice was achieved by tail vein injection of AAV8-*Prdx1* (1.1×10^{12} vg/mouse). Four weeks after injection, the mice were treated with CCl_4 using the same protocol as described above.

All mice-related experiments were carried out following the Guide for the Care and Use of Laboratory Animals (Eighth Edition, 2011) and were approved by the Animal Care and Use Committee of University of Chinese Academy of Sciences (UCAS-A-20220923).

2.2. Biochemical and histological analyses

Serum alanine aminotransferase (ALT) and aspartate aminotransferase (AST) levels were measured using commercial kits. Serum ADMA levels and liver 4-hydroxynonenal (4-HNE) and 3′-nitrotyrosine (3′-NT) were measured with respective ELISA kits. Liver paraffin sections (5 μm) were stained with hematoxylin and eosin (H&E), Masson, and TUNEL kits to assess histopathological damage, fibrosis, and apoptosis, respectively. Frozen liver sections (4 μm) were stained with dihydroethidium (DHE) to evaluate the degree of oxidative stress.

2.3. Cell culture and assays

HEK293, 293T and HepG2 cells were obtained from the Cell Bank of the Institute of Biochemistry and Cell Biology (Shanghai, China). DMEM containing 10% FBS and 1% penicillin and streptomycin was used for cell culture. As previously described [23], the MTT method was used for measuring cell viability. DCFH-DA and DHE were used to measure intracellular ROS and superoxide levels, respectively. Notable, although DCFH-DA is a wildly used fluorescent probe, it has several limitations [24]. The ratio of reduced GSH to oxidized GSH (GSSG) were measured by commercial kit (#S0053, Beyotime Biotechnology, Shanghai, China).

To perform the bimolecular fluorescence complementation (BiFC) assay, cells were grown in glass-bottom plates, and the target plasmids were transfected using Lipofectamine 3000 at approximately 50% cell density. After 24 h, the medium was replaced with a fresh medium, and the cells were treated with PBS, 100 μM H_2O_2 or 5 mM NAC for 2 h. Then, BiFC signals were obtained via laser confocal microscopy (LSM880, Zeiss, Germany) at an excitation wavelength of 488 nm/emission wavelength of 525 nm.

2.4. Coimmunoprecipitation

HEK293 cells were cotransfected with the indicated plasmids for coimmunoprecipitation (co-IP) assays. The cells were lysed with native lysis buffer (#R0030, Solarbio Science & Technology Co., Ltd., Beijing, China) containing protease and phosphatase inhibitor cocktail at 4 °C for 30 min. The lysates were centrifuged at 12,000×*g* for 10 min and 500 μl of the supernatant was preprocessed with 20 μl of protein A/G magnetic beads (#B23201, Bimake, USA) and 1 μg of the corresponding IgG antibody at 4 °C for 1 h. Anti-Myc magnetic beads were incubated with the supernatants at 4 °C overnight. The magnetic beads were then washed with a cold washing buffer (20 mM Tris-HCl, pH 7.4, 150 mM NaCl, 1 mM EDTA, 0.5% Triton X-100, and protease and phosphatase inhibitor cocktail) three times and boiled with 2 × SDS loading buffer prior to western blot analysis.

2.5. Plasmid construction and virus packaging

PRDX1 (NM_001202431.2), *DDAH1* (NM_012137.4) and *SRXN1* (NM_080725.3) were subcloned into the expression vectors (e.g. pQCXIH and pCMV-C-Myc/mcherry), respectively. Short hairpin RNA (shRNA) sequences targeting human *DDAH1* (5′-GGGCCTAACCT-GATCGCAATT-3′), *PRDX1* (5′-GGCCACAGCTGTTATGCCAGA-3′) and *SRXN1* (5′-GTTGGCGGGGTCCAACACGGA-3′) were constructed in the lentiviral vector PLKO.1 (Addgene plasmid #10878 [25]). The obtained pQCXIH expression vectors and shRNA vectors were used for subsequent retroviral and lentiviral packaging, respectively. To perform the BiFC assay, DDAH1^{WT} and the DDAH1^{C274A} mutant were subcloned into the pBiFC-VC155 vector. PRDX1 and SRXN1 were subcloned into the

pBiFC-VN173 vector. The sequences of the primers used for plasmid construction are listed in Table S2.

Site-directed mutagenesis kits were used to generate DDAH1 mutations at the His^{173}, Cys^{274} and Cys^{275} sites and PRDX1 mutations at the Cys^{52} and Cys^{173} sites. The mutations were confirmed by DNA sequencing. The sequences of the primers used for site-specific mutagenesis are listed in Table S3.

2.6. Quantitative real-time PCR and western blotting

Total RNA was extracted from livers using the TRIzol reagent and reverse-transcribed with the PrimeScript RT reagent. Subsequently, real-time PCR was performed using TB Green Premix Ex Taq II on a QuantStudio 7 PCR detection system (Thermo Fisher Scientific, USA). Relative expression was calculated by the $2^{-\triangle\triangle Ct}$ method with normalization to the 18S rRNA gene expression. The primer sequences are listed in

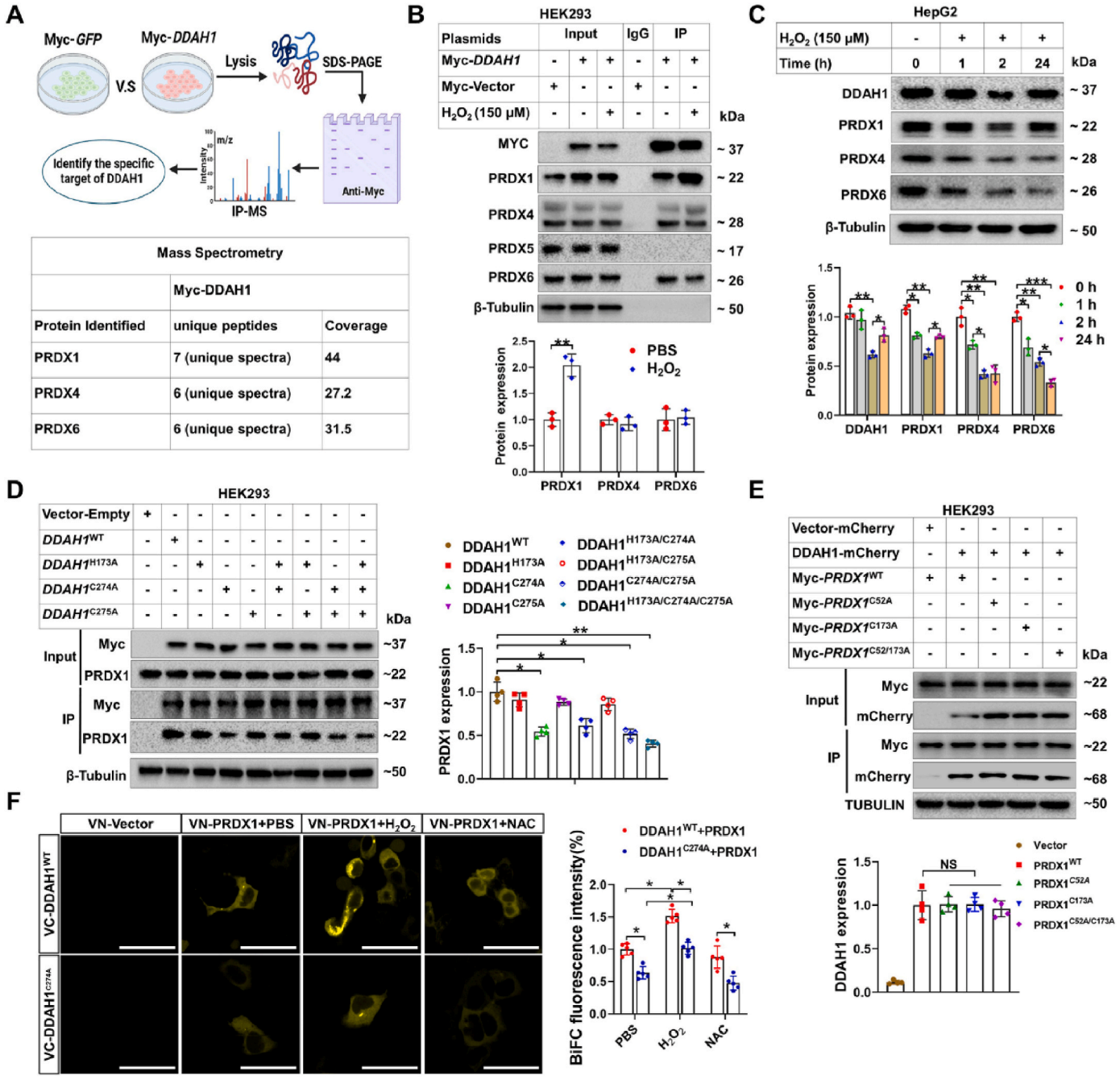

Fig. 1. PRDX1 is one of the identified proteins that interact with DDAH1. (A) The experimental processes are illustrated in the diagram. Mass spectrometry analysis identified three PRDXs in the myc-DDAH1 immunoprecipitates. (B) Lysates of HEK293 cells transfected with myc-*DDAH1* and treated with or without H_2O_2 for 2 h were subjected to immunoprecipitation, and the resulting immunoprecipitates (IP) and cell lysates (Input) were analyzed by Western blotting. (C) HepG2 cells were exposed to 150 μM H_2O_2 for 1, 2 and 24 h, and the cell lysates were examined by Western blotting. (D) HEK293 cells transfected with WT or mutant DDAH1 plasmids were subjected to co-IP analysis. (E) HEK293 cells were transfected with DDAH1 tagged with mCherry plus WT or mutant PRDX1 plasmids tagged with myc for 24 h. The resulting cell lysates were analyzed by co-IP. (F) HEK293 cells were transfected with pBiFC-VN173-*PRDX1,* pBiFC-VC155-*DDAH1* or pBiFC-VC155-*DDAH1*^{C274A} for 24 h and treated with or without 100 μM H_2O_2 or 5 mM NAC for 2 h. Fluorescence images were taken by confocal microscopy. Scale bar = 50 μm. The values are expressed as the means ± SDs. In Fig. B–C, N = 3; in Fig. D–E, N = 4; in Fig. F, N = 5; *p < 0.05; **p < 0.01; ***p < 0.001; NS, not significant.

Table S4.

Protein was extracted from pulverized livers and scraped cells on ice for 30 min using a lysis buffer containing 150 mM NaCl, 50 mM Tris-HCl, 100 μg/ml PMSF, a protease and phosphatase inhibitor cocktail and 1% Triton X-100. The lysates were centrifuged at 12,000×*g* for 20 min at 4 °C, and the supernatants were subjected to western blot analysis. The detailed procedures were described in our previous study [22], and the information for the primary antibodies is provided in Table S1.

2.7. Data and statistical analysis

All the values are expressed as the means ± SDs and were analyzed with GraphPad Prism 8 (GraphPad Software, Inc., San Diego, CA, USA). The statistical significance of differences between two groups was analyzed using the unpaired two-tailed Student's *t*-test. One- or two-way ANOVA with Tukey's correction was used for multiple comparisons among the groups. A value of $p < 0.05$ was considered to indicate statistical significance.

3. Results

3.1. PRDX1 was shown to interact with DDAH1

DDAH1 has been found to interact with eNOS to maintain compartmentalized NO signaling in cardiomyocytes [26]. To investigate whether DDAH1 interacts with certain proteins to affect the cellular redox state, lysates of HEK293 cells transfected with the Myc epitope-tagged DDAH1 (Myc-*DDAH1*) or Myc-*GFP* expression construct were immunoprecipitated with anti-Myc magnetic beads. The immunoprecipitates were separated by SDS−PAGE and then analyzed by mass spectrometry. PRDX1, PRDX4, and PRDX6 were identified in the immunoprecipitates, and the specific peptide coverage was 44%, 27.2% and 31.6%, respectively (Fig. 1A). The covered peptide sequences are shown in Fig. S1. Co-IP analysis confirmed that DDAH1 interacted with PRDX1, PRDX4, and PRDX6 but not with PRDX5. Interestingly, when the cells were incubated with 150 μM H_2O_2 for 2 h, more PRDX1 was detected in the Myc-DDAH1 immunoprecipitates, while the PRDX4 and PRDX6 levels were not affected (Fig. 1B). Moreover, the reciprocal immunoprecipitation assay showed that H_2O_2 increased the DDAH1 content in the Myc-PRDX1 immunoprecipitates (Fig. S2). To investigate the dynamic changes in protein expression during oxidative stress, we treated HepG2 cells with H_2O_2 for 1, 2 and 24 h. After 2 h of treatment, the expression of DDAH1 and PRDX1/4/6 was significantly reduced. When the treatment time was extended to 24 h, the reductions in the expression of DDAH1 and PRDX1 were decreased. However, the expression of PRDX4 was unchanged, and that of PRDX6 further decreased (Fig. 1C).

Cys^{274} and His^{173} were identified as critical active site residues in human DDAH1. Alanine mutations at Cys^{274} and His^{173} have no detectable activity, while the C275A mutation results in a k_{cat} value of approximately half of that of the WT protein [16]. To elucidate whether the active site residues are involved in the interaction between DDAH1 and PRDX1, we generated 7 mutants, H173A, C274A, C275A, H173A/C274A, H173A/C275A, C274A/C275A, and H173A/C274A/C275A. The effect of mutations on DDAH1 activity was indirectly determined by measuring the intracellular ADMA levels. In ADMA treated HEK293 cells, transfection with WT DDAH1 significantly decreased intracellular ADMA levels, while the DDAH1 mutations had no obvious effects (Fig. S3). Co-IP analysis of the immunoprecipitates revealed that the mutation at Cys^{274} significantly decreased PRDX1 levels, but the mutations at His^{173} and Cys^{275} had no obvious effects on the PRDX1 content, indicating that Cys^{274} in DDAH1 is important for its interaction with PRDX1 (Fig. 1D).

PRDX1 is a typical 2-Cys PRDX protein that uses redox-active cysteines to reduce peroxides [27,28]. Similarly, we mutated Cys^{52} and Cys^{173} in PRDX1 and generated three mutants: C52A, C173A and C52/C173A. Co-IP analysis of the immunoprecipitates of WT PRDX1 and mutated PDRX1 revealed similar DDAH1 levels, indicating that mutations at Cys^{52} and Cys^{173} have no obvious effect on the PRDX1-DDAH1 interaction (Fig. 1E).

Next, we performed a BiFC assay to visualize the effect of the redox state on the interaction between DDAH1 and PRDX1 in living cells. HEK293 cells cotransfected with pBiFC-VC155-*DDAH1* and pBiFC-VN173-*PRDX1* exhibited strong BiFC fluorescence signals, indicating that DDAH1 indeed interacts with PRDX1. The signal was further increased by H_2O_2 treatment (100 μM, 2 h) but not by NAC treatment (5 mM, 2 h). When pBiFC-VC155-$DDAH1^{Cys274}$ was cotransfected, the intensity of the BiFC fluorescent signals decreased in PBS-, H_2O_2- and NAC-treated cells (Fig. 1F).

3.2. PRDX1 protects against H_2O_2-induced downregulation of DDAH1

In HepG2 cells, H_2O_2 dose-dependently decreased cell viability and increased intracellular ROS and ADMA levels (Fig. S4). To elucidate the effect of the DDAH1-PRDX1 interaction on cellular redox homeostasis, we stably transfected HepG2 cells with a sh*PRDX1* lentiviral vector or a shRNA lentiviral vector targeting a scrambled sequence (shScr). Under basal conditions, PRDX1 knockdown slightly but significantly increased the intracellular ROS and ADMA levels. In response to H_2O_2 treatment (150 μM, 24 h), PRDX1 knockdown resulted in a greater cell viability loss and greater increases in intracellular ADMA, ROS and superoxide levels (Fig. 2A–D). H_2O_2 treatment significantly decreased the GSH/GSSG ratio, which was aggravated by PRDX1 knockdown (Fig. 2E). On the other hand, overexpression of PRDX1 (PQ-*PRDX1*) via infection with the retroviral vector pQCXIH-*PRDX1* decreased the intracellular ADMA and ROS levels in control cells. PRDX1 overexpression increased cell viability and decreased the intracellular ADMA, ROS and superoxide levels in H_2O_2-treated cells (Fig. 2F–I). Overexpression of PRDX1 also attenuated the H_2O_2-induced decreases in GSH/GSSG ratio (Fig. 2J).

Western blot analysis revealed that stable transfection of sh*PRDX1* decreased the expression of the target gene by ~60%. PRDX1 knockdown increased the expression of oxidized PRDXs (PRDX-SO_3) and SRXN1 in control cells and exacerbated the H_2O_2-induced downregulation of DDAH1 and upregulation of PRDX-SO_3 (Fig. 2K). Overexpression of PRDX1 decreased PRDX-SO_3 expression under basal conditions and significantly attenuated the H_2O_2-induced downregulation of DDAH1 and SRXN1 (Fig. 2L). To determine whether the active site residues (Cys^{52} and Cys^{173}) in PRDX1 are involved in the protection of DDAH1 under oxidative stress conditions, we transfected HEK293 cells with Myc-tagged WT and mutant PRDX1 expression vectors and then treated the cells with 100 μM H_2O_2 for 24 h. As shown in Fig. 2M, downregulation of DDAH1 could be attenuated only by overexpression of WT PRDX1 but not by any of the PRDX1 mutants. Overexpression of the Myc-$PRDX1^{C52A/C173A}$ construct caused an even greater decrease in DDAH1 expression in H_2O_2-treated cells (Fig. 2M). Taken together, these results suggested that PRDX1 could preserve DDAH1 expression and activity under conditions of oxidative stress.

3.3. SRXN1 interacts with DDAH1 and protects its expression and activity

Since the results of the STRING database (https://string-db.org/) suggest that PRDX and SRXN1 interact at the protein level (Fig. S5), we transfected HEK293 cells with the myc-*DDAH1* construct and performed co-IP analysis. The results showed that SRXN1 was present in the Myc-DDAH1 immunoprecipitates and that its content increased with H_2O_2 treatment (150 μM, 2 h), suggesting that there was a direct interaction between SRXN1 and DDAH1 and that this interaction could be enhanced by oxidative stress (Fig. 3A). Similarly, we cotransfected HEK293T cells with the pBiFC-VN173-*SRXN1,* pBiFC-VC155-*DDAH1* and pBiFC-VC155-$DDAH1^{C274A}$ plasmids for BiFC verification. The results showed that the interaction between SRXN1 and DDAH1 was enhanced by H_2O_2 treatment but was not affected by NAC treatment or the C274A mutation

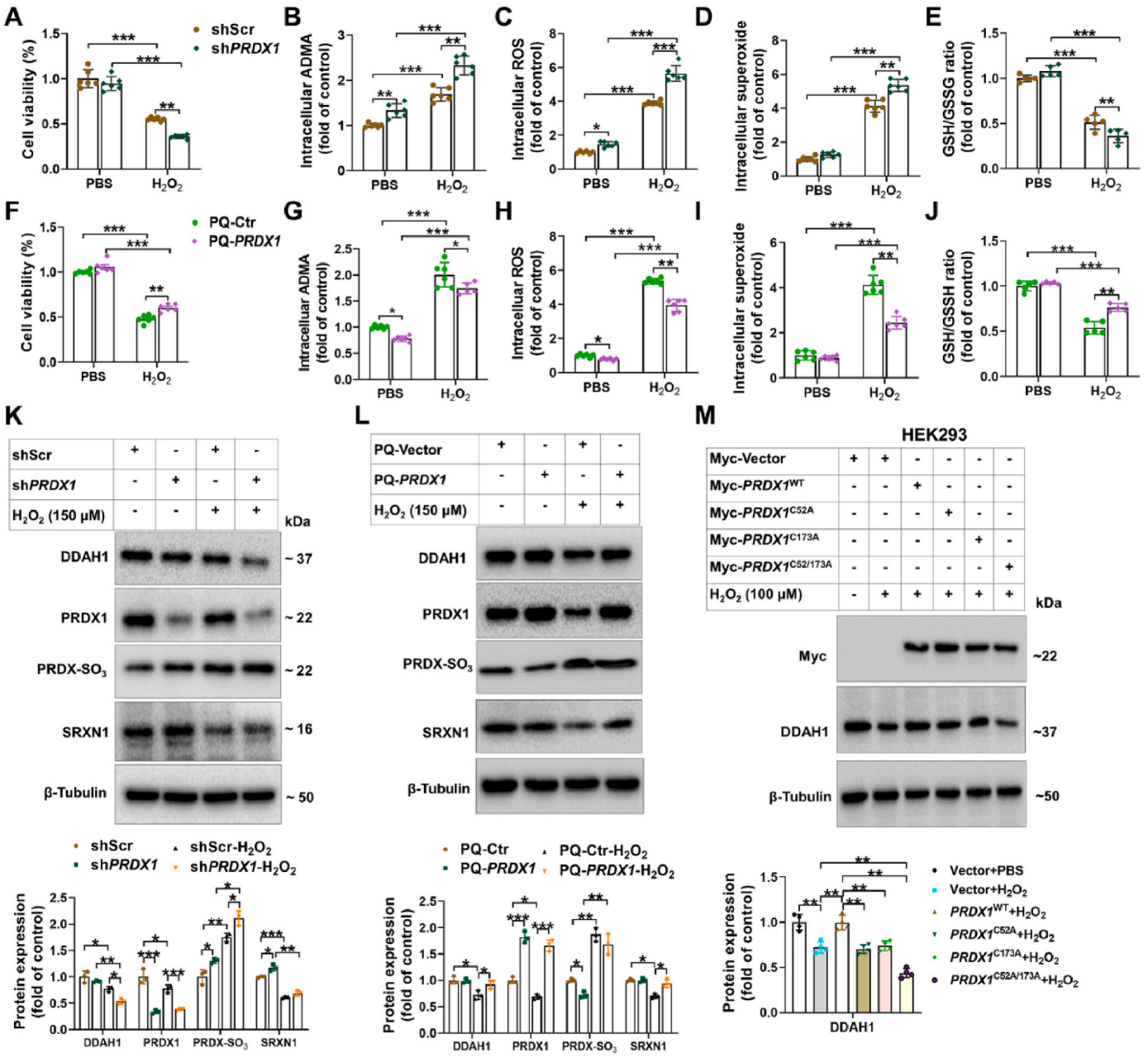

Fig. 2. PRDX1 preserves cell viability, DDAH1 expression, and redox homeostasis in H_2O_2-treated cells. (A–E) HepG2 cells stably transfected with a shRNA lentiviral vector targeting a scrambled sequence (shScr) or PRDX1 (sh*PRDX1*) were treated with or without 150 μM H_2O_2 for 24 h. Then, cell viability (A) was measure by MTT method. The Intracellular ADMA levels were measure by ELISA kit (B). The intracellular reactive oxygen species (ROS) (C) and superoxide (D) levels were measured by DCFH-DA and dihydroethidium (DHE), respectively. The GSH/GSSG ratio was measured by commercial kit(E). (F–J) HepG2 cells stably transfected with the empty retroviral vector (PQ-Ctr) or the PRDX1 expression vector (PQ-*PRDX1*) were incubated with or without 150 μM H_2O_2 for 24 h. Cell viability (F) and intracellular ADMA (G), ROS (H), and superoxide (I) levels and GSH/GSSG ratio (J) were subsequently measured. (K) HepG2 cells stably transfected with shScr or sh*PRDX1* were examined by western blotting. (L) Lysates of control and PRDX1-overexpressing cells were subjected to western blot analysis. (M) HEK293 cells were transfected with WT or mutant PRDX1 expression vectors and then incubated with 100 μM H_2O_2 for 24 h. The cell lysates were examined by western blotting. The values are expressed as the means ± SDs. In Fig. A–D and F–I, N = 6; in Fig. E and J, N = 5; in Fig. K–M, N = 3; *p < 0.05; **p < 0.01; ***p < 0.001.

(Fig. 3B).

To determine whether SRXN1 affects DDAH1 expression and activity in response to oxidative stress, we first stably transfected HepG2 cells with sh*SRXN1*. Under basal conditions, SRXN1 knockdown increased the intracellular ADMA and ROS levels. After H_2O_2 treatment (150 μM, 24 h), SRXN1 elimination further decreased cell viability and increased intracellular ADMA, ROS and superoxide levels in H_2O_2-treated cells (Fig. 3C–F). SRXN1 knockdown also exacerbated H_2O_2-induced decrease in GSH/GSSG ratio (Fig. 3G). We then overexpressed SRXN1 (PQ-*SRXN1*) in HepG2 cells via transfection with the retroviral pQCXIH-*SRXN1* vector. SRXN1 overexpression attenuated the decrease in cell viability of H_2O_2-treated cells and decreased the intracellular ADMA, ROS and superoxide levels in control and H_2O_2-treated cells (Fig. 3H–K). SRXN1 overexpression also attenuated the decrease in GSH/GSSG ratio after H_2O_2 treatment (Fig. 3L).

Western blot analysis revealed that SRXN1 knockdown caused significant decreases in DDAH1 and PRDX1 expression and increases in PRDX-SO_3 expression in control and H_2O_2-treated HepG2 cells (Fig. 3M). SRXN1 overexpression significantly attenuated the H_2O_2-induced downregulation of DDAH1 and PRDX1 and upregulation of

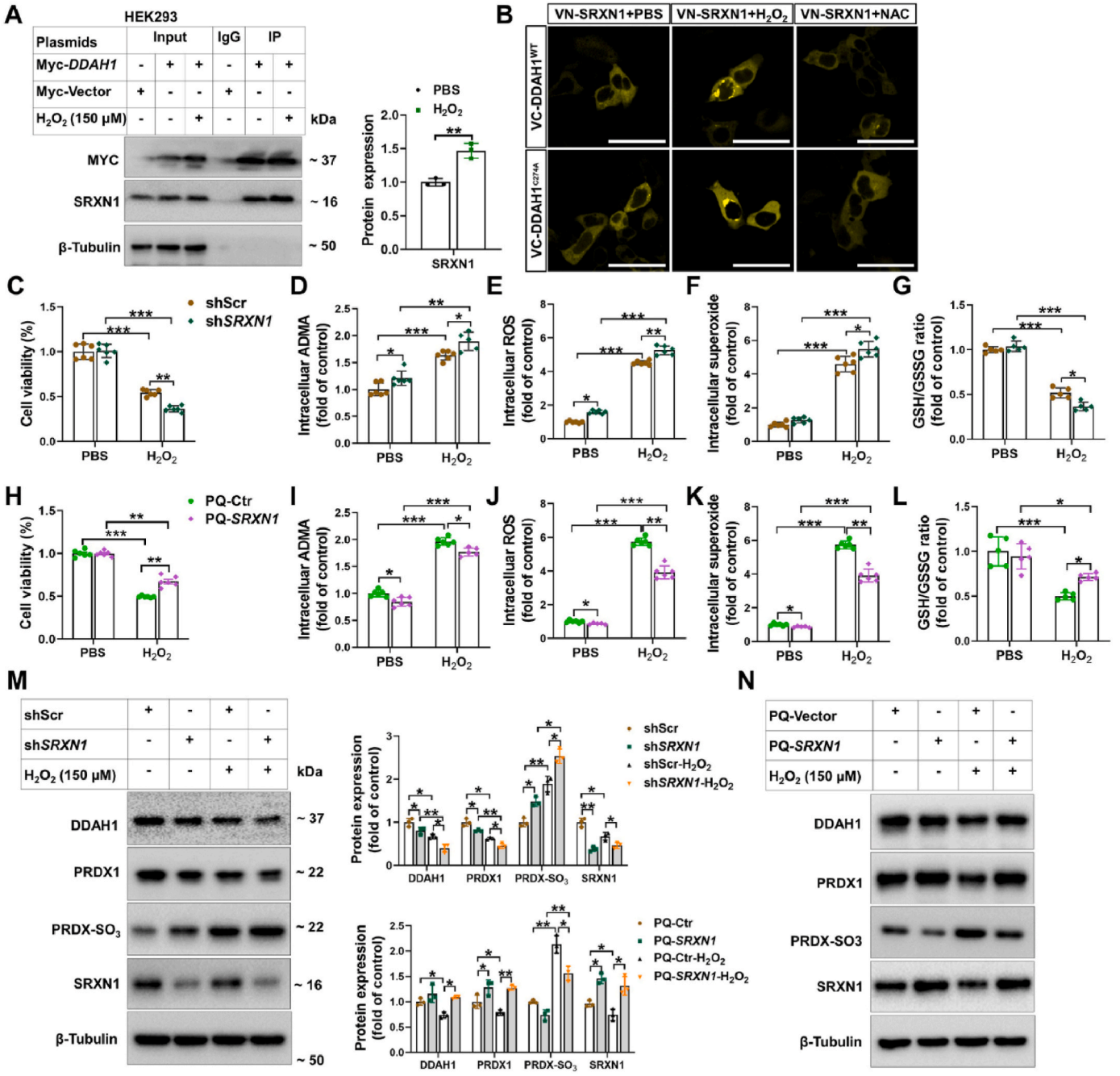

Fig. 3. SRXN1 interacts with DDAH1, attenuates the loss of cell viability, and maintains DDAH1 expression and redox homeostasis in H_2O_2-treated cells. (A) HEK293 cells were transfected with myc-*DDAH1* and treated with or without 150 μM H_2O_2 for 2 h, followed by co-IP analysis. (B) HEK293 cells cotransfected with pBiFC-VN173-*SRXN1* and pBiFC-VC155-*DDAH1* or pBiFC-VC155-*DDAH1*^{C274A} were treated with PBS, H_2O_2 (100 μM) or NAC (5 mM) for 2 h, and then BiFC images were obtained by confocal microscopy. Scale bar = 50 μm. (C–G) HepG2 cells stably transfected with shScr or sh*SRXN1* were treated with or without 150 μM H_2O_2 for 24 h. Then, cell viability (C) and intracellular ADMA (D), ROS (E), and superoxide (F) levels were measured. The GSH/GSSG ratio in control and H_2O_2-treated cells were measured (G). (H–L) HepG2 cells stably transfected with the empty retroviral vector (PQ-Ctr) or SRXN1 expression vector (PQ-*SRXN1*) were incubated with or without 150 μM H_2O_2 for 24 h. Cell viability (H), intracellular ADMA (I), ROS (J), and superoxide (K) levels and GSH/GSSG ratio (L) were subsequently measured. (M, N) After H_2O_2 treatment (150 μM, 24 h), control and SRXN1-depleted or SRXN1-overexpressing cells were collected, and cell lysates were examined by western blotting. The values are expressed as the means ± SDs. In Fig. A, M and N, N = 3; in Fig. C–F and H–K, N = 6; in Fig. G and L, N = 5; *p < 0.05; **p < 0.01; ***p < 0.001.

PRDX-SO_3 (Fig. 3N). Taken together, these results suggested that SRXN1 not only functioned as a reductase of oxidized PRDXs but also maintained the expression and activity of DDAH1 under conditions of oxidative stress.

3.4. *DDAH1 affects redox homeostasis and PRDX1 and SRXN1 expression under oxidative stress conditions*

To determine whether DDAH1 also affects the redox state and PRDX1/SRXN1 expression under oxidative stress conditions, we stably transfected HepG2 cells with a sh*DDAH1* lentivirus or the retroviral vector pQCXIH-*DDAH1* to knock down or overexpress DDAH1 (PQ-

DDAH1), respectively. Under control conditions, DDAH1 knockdown increased the intracellular ADMA, ROS, and superoxide levels. In response to H_2O_2 treatment (150 μM, 24 h), DDAH1 knockdown resulted in a greater cell viability loss and greater increases in the intracellular levels of ADMA, ROS, and superoxide (Fig. 4A–D). DDAH1 knockdown also exacerbated the decrease in GSH/GSSG ratio in H_2O_2-treated cells (Fig. 4E). On the other hand, DDAH1 overexpression significantly decreased the intracellular ADMA and ROS levels in control cells. DDAH1 overexpression attenuated the cell viability loss and decreased the intracellular ADMA, ROS, and superoxide levels in H_2O_2-treated cells (Fig. 4F–I). The H_2O_2-induced decrease in GSH/GSSG ratio were attenuated by DDAH1 overexpression (Fig. 4J).

Western blot analysis revealed that stable transfection of cells with sh*DDAH1* caused a more than 90% decrease in DDAH1 expression. Interestingly, DDAH1 knockdown increased the expression of PRDX1 and SRXN1 in control and H_2O_2-treated cells but had no obvious effect on the expression of PRDX-SO_3 (Fig. 4K). DDAH1 overexpression significantly attenuated H_2O_2-induced upregulation of PRDX-SO_3 and downregulation of PRDX1 and SRXN1 (Fig. 4L). To determine whether the active site residues in DDAH1 are needed for the maintenance of PRDX1 and SRXN1 expression in H_2O_2-treated cells, HEK293 cells were transfected with the WT and mutant DDAH1 constructs and then incubated with 100 μM H_2O_2 for 24 h. Western blot analysis revealed that only the WT and DDAH1^{H173A} mutant constructs could attenuate the H_2O_2-induced downregulation of PRDX1. Other mutations, including DDAH1^{C274A}, DDAH1^{C275A}, DDAH1$^{H173A/C274A}$, DDAH1$^{H173A/C275A}$, DDAH1$^{C274A/C275A}$ and DDAH1$^{H173A/C274A/C275A}$, had no effect on the expression of PRDX1 or SRXN1 in H_2O_2-treated cells (Fig. 4M), indicating that Cys^{274} and Cys^{275} in DDAH1 are important for the regulation of PRDX1 and SRXN1 expression under oxidative stress conditions. We also determined the effects of these mutations on intracellular ROS levels in HEK293 cells. In unstressed cells, transfection with the WT or DDAH1-mutant constructs had no obvious effect on intracellular ROS levels. In H_2O_2-treated cells, the overexpression of DDAH1^{WT} or DDAH1^{H173A} significantly decreased the ROS levels. Although overexpression of the DDAH1^{C274A} and DDAH1^{C275A} mutants also decreased the intracellular ROS levels, the degree of ROS generation was much weaker than that with the WT DDAH1 plasmid. Other mutations, including DDAH1$^{H173A/C274A}$, DDAH1$^{H173A/C275A}$, DDAH1$^{C274A/C275A}$ and DDAH1$^{H173A/C274A/C275A}$, failed to attenuate H_2O_2-induced oxidative stress (Fig. 4N). In HepG2 cells, transient overexpression of DDAH1^{C274A} did not affect cell viability or intracellular ROS levels in control and H_2O_2-treated cells (Fig. 4O-P), suggesting that Cys^{274} is important for DDAH1-mediated protection against oxidative stress.

3.5. *DDAH1 ameliorates CCl_4-induced liver injury, oxidative stress, and cell death*

To study the *in vivo* effects of DDAH1 on PRDX1 and SRXN1 expression under oxidative stress conditions, we treated WT, *Ddah1*$^{-/-}$, and DDAH1-TG mice with CCl_4 via intraperitoneal injection to induce liver oxidative stress. The experimental process is illustrated in Fig. 5A. After CCl_4 treatment, the serum AST and ALT levels significantly increased, and these increases were exacerbated in *Ddah1*$^{-/-}$ mice but attenuated in DDAH1-TG mice (Fig. 5B and C). *Ddah1* deletion increased the serum ADMA concentration in control mice and further aggravated the CCl_4-induced increase in the serum ADMA concentration. However, there were no significant changes in the serum ADMA level in the DDAH1-TG mice after CCl_4 treatment (Fig. 5D). H&E, Masson, DHE and TUNEL staining revealed that CCl_4 caused more pathological alterations (for example, inflammatory cell infiltration, centrilobular hepatic necrosis, and ballooning degeneration), fibrosis, superoxide generation, and apoptosis in the livers of *Ddah1*$^{-/-}$ mice than in those of WT mice. CCl_4-induced pathological lesions, fibrosis, oxidative stress and apoptosis were significantly improved in the livers of DDAH1-TG mice (Fig. 5E–H). Furthermore, CCl_4-induced increases in the liver 4-HNE and 3′-NT levels were greater in *Ddah1*$^{-/-}$ mice than in WT mice (Fig. 5I and J). CCl_4 significantly increased the mRNA levels of collagen I, collagen III, TNFα and IL-1β in the livers of mice of the three genotypes. Meanwhile, the increases in the expression of the liver fibrotic and inflammatory genes were exacerbated in *Ddah1*$^{-/-}$ mice but alleviated in DDAH1-TG mice (Fig. 5K-N).

DDAH1 expression was completely undetected in the livers of *Ddah1*$^{-/-}$ mice. CCl_4 decreased the expression of liver DDAH1 in both WT and DDAH1-TG mice. However, liver DDAH1 expression was greater in DDAH1-TG mice than in WT mice. Treatment with CCl_4 decreased PRDX1 and Bcl-2 expression but increased that of PRDX-SO_3, SRXN1, and Bax in the livers of WT and *Ddah1*$^{-/-}$ mice. However, *Ddah1*$^{-/-}$ mice exhibited lower levels of liver PRDX1, SRXN1, and Bcl-2 and higher levels of liver PRDX-SO_3 and Bax than did WT mice. Although CCl_4 also decreased PRDX1 expression in the livers of DDAH1-TG mice, the difference was not significant. The CCl_4-induced downregulation of Bcl-2 and upregulation of PRDX-SO_3 and Bax were attenuated. However, the upregulation of SRXN1 was further enhanced by the overexpression of DDAH1 (Fig. 5O). CCl_4 also increased PRDX4 expression and decreased PRDX6 expression in mice of the three genotypes. However, PRDX4 upregulation was attenuated in the livers of *Ddah1*$^{-/-}$ mice (Fig. S6A).

3.6. *Hepatocyte-specific deletion of Ddah1 exacerbates CCl_4-induced hepatotoxicity and downregulation of PRDX1*

To elucidate whether hepatic DDAH1 affects hepatotoxicity of CCl_4 and the PRDX1/SRXN1 pathway, we treated *Ddah1*^{HKO} and *Ddah1*$^{f/f}$ mice with CCl_4 using the same protocol. After treatment, *Ddah1*^{HKO} mice exhibited higher AST and ALT levels than did *Ddah1*$^{f/f}$ mice (Fig. 6A and B). Although *Ddah1*^{HKO} mice had higher serum ADMA levels than *Ddah1*$^{f/f}$ mice under basal conditions, this difference was diminished after CCl_4 treatment (Fig. 6C). As revealed by H&E, Masson, DHE and TUNEL staining, CCl_4 treatment caused more liver injury, fibrosis, superoxide generation, and apoptotic cells in *Ddah1*^{HKO} mice than in *Ddah1*$^{f/f}$ mice (Fig. 6D–G). The *Ddah1*^{HKO} mice also showed the aggravation of CCl_4-induced increases in liver 4-HNE levels and in mRNA levels of collagen I, collagen III, TNFα and IL-1β (Fig. 6H-L). Western blot analysis revealed that specific deletion of *Ddah1* in hepatocytes exacerbated the downregulation of PRDX1 and Bcl-2 and the upregulation of PRDX-SO_3 and Bax and attenuated the upregulation of SRXN1 and PRDX4 in the livers of mice treated with CCl_4 (Fig. 6M, Fig. S6). Liver PRDX6 expression was not affected by hepatic *Ddah1* deletion in oil- or CCl_4-treated mice (Fig. S6B).

3.7. *Hepatic overexpression of PRDX1 alleviates CCl_4-induced hepatotoxicity and diminishes the effect of Ddah1 deficiency*

To determine whether hepatocyte-specific overexpression of PRDX1 could maintain DDAH1 expression and activity *in vivo*, we treated CCl_4-exposed WT and *Ddah1*$^{-/-}$ mice with AAV8-*Prdx1* via tail vein injection. WT mice that received AAV8-*GFP* injection were used as controls. PRDX1 overexpression significantly decreased the serum AST, ALT, and ADMA levels in CCl_4-treated mice (Fig. 7A–C). Interestingly, the differences in the serum AST and ALT levels between the WT and *Ddah1*$^{-/-}$ mice were reduced by PRDX1 overexpression (Fig. 7A and B). Furthermore, PRDX1 overexpression similarly ameliorated CCl_4-induced pathological changes, fibrosis, superoxide generation, and apoptosis in the livers of WT and *Ddah1*$^{-/-}$ mice (Fig. 7D–G). After CCl_4 treatment, the liver from *Ddah1*$^{-/-}$ mice exhibited higher levels of 3′-NT levels and 4-HNE levels than WT livers. Overexpression of PRDX1 decreased 3′-NT and 4-HNE levels and mRNA levels of *collagen I*, *collagen III*, *TNF-α* and *IL-1β* in the livers of CCl_4-treated mice (Fig. 7H-M). After PRDX1 was overexpressed, CCl_4-treated WT and *Ddah1*$^{-/-}$ mice exhibited similar liver fibrosis areas, superoxide generation, apoptotic cell numbers, 3′-NT and 4-HNE levels and mRNA levels of the fibrotic and inflammatory genes (Fig. 7D-M). Western blot analysis of the livers of mice treated

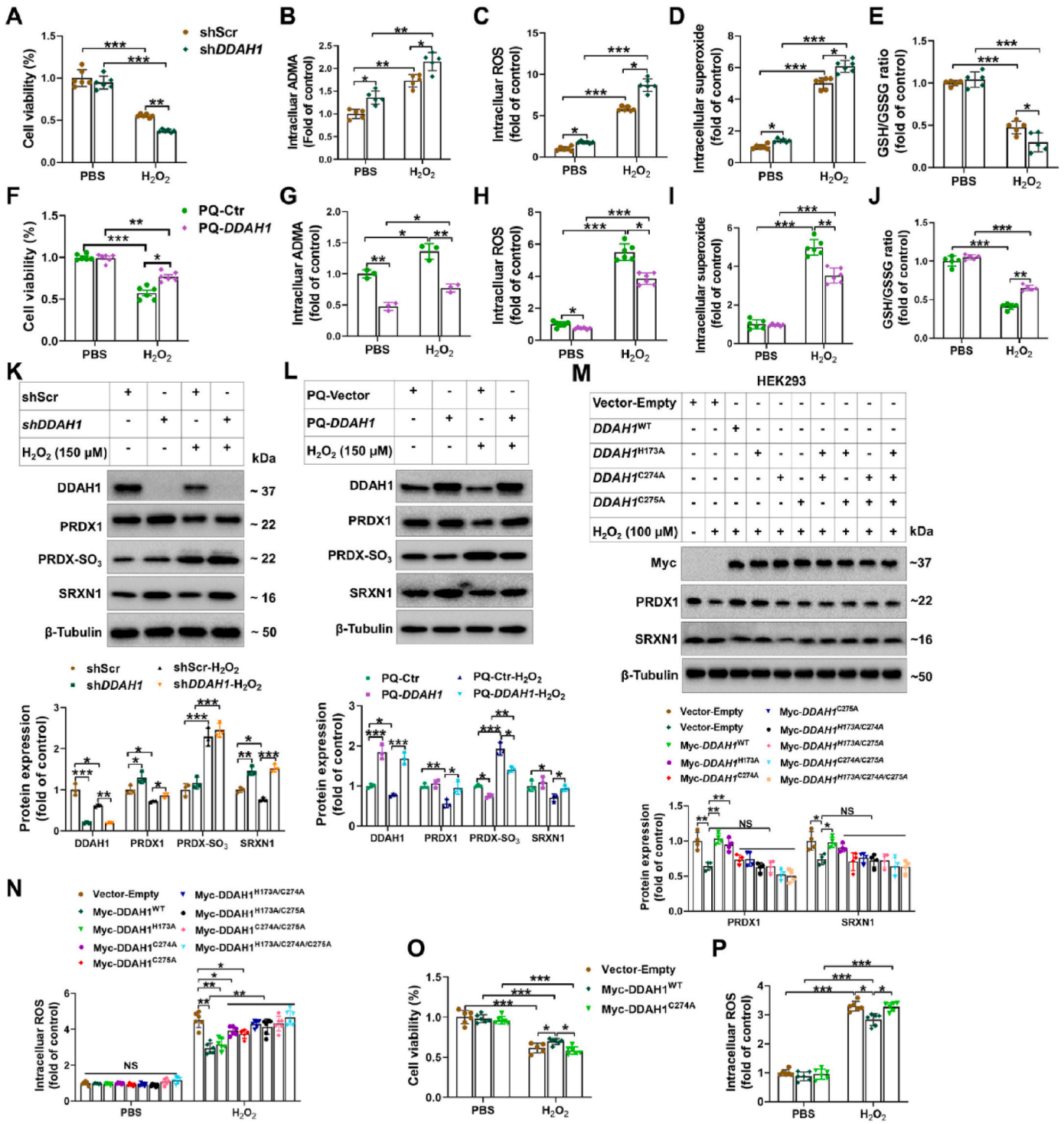

Fig. 4. DDAH1 maintains redox homeostasis and PRDX1/SRXN1 expression in H_2O_2-treated cells. (A–E) HepG2 cells stably transfected with ShScr or sh*DDAH1* were treated with PBS or 150 μM H_2O_2 for 24 h. Then, cell viability (A), intracellular ADMA (B), ROS (C) and superoxide (D) levels, and GSH/GSSG ratio (E) were measured. (F–J) HepG2 cells stably transfected with the empty retroviral vector (PQ-Ctr) or DDAH1 expression vector (PQ-*DDAH1*) were incubated with or without 150 μM H_2O_2 for 24 h. Cell viability (F), intracellular ADMA (G), ROS (H) and superoxide (I) levels, and GSH/GSSG ratio (J) were subsequently measured. (K, L) Lysates from control and H_2O_2-treated DDAH1-depleted and DDAH1-overexpressing cells were examined by western blotting. (M) HEK293 cells transfected with the WT or mutant DDAH1 constructs and treated with or without H_2O_2 (100 μM, 2 h) were analyzed by western blotting. (N) DCFH-DA was used to determine ROS levels in HEK293T cells transfected with different mutants and treated with or without H_2O_2 (100 μM) for 24 h HepG2 cells transfected with the empty vector or DDAH1 WT or C274 mutant lentivirus were incubated with PBS or H_2O_2 for 24 h. Then, cell viability (O) and intracellular ROS levels (P) were measured. The values are expressed as the means ± SDs. In Fig. A–D, F, H–I, O–P, N = 6; In Fig E, J, N = 5; in Fig. G, K, L and M, N = 3; in Fig. N, N = 4; *p < 0.05; **p < 0.01; ***p < 0.001; NS, not significant.

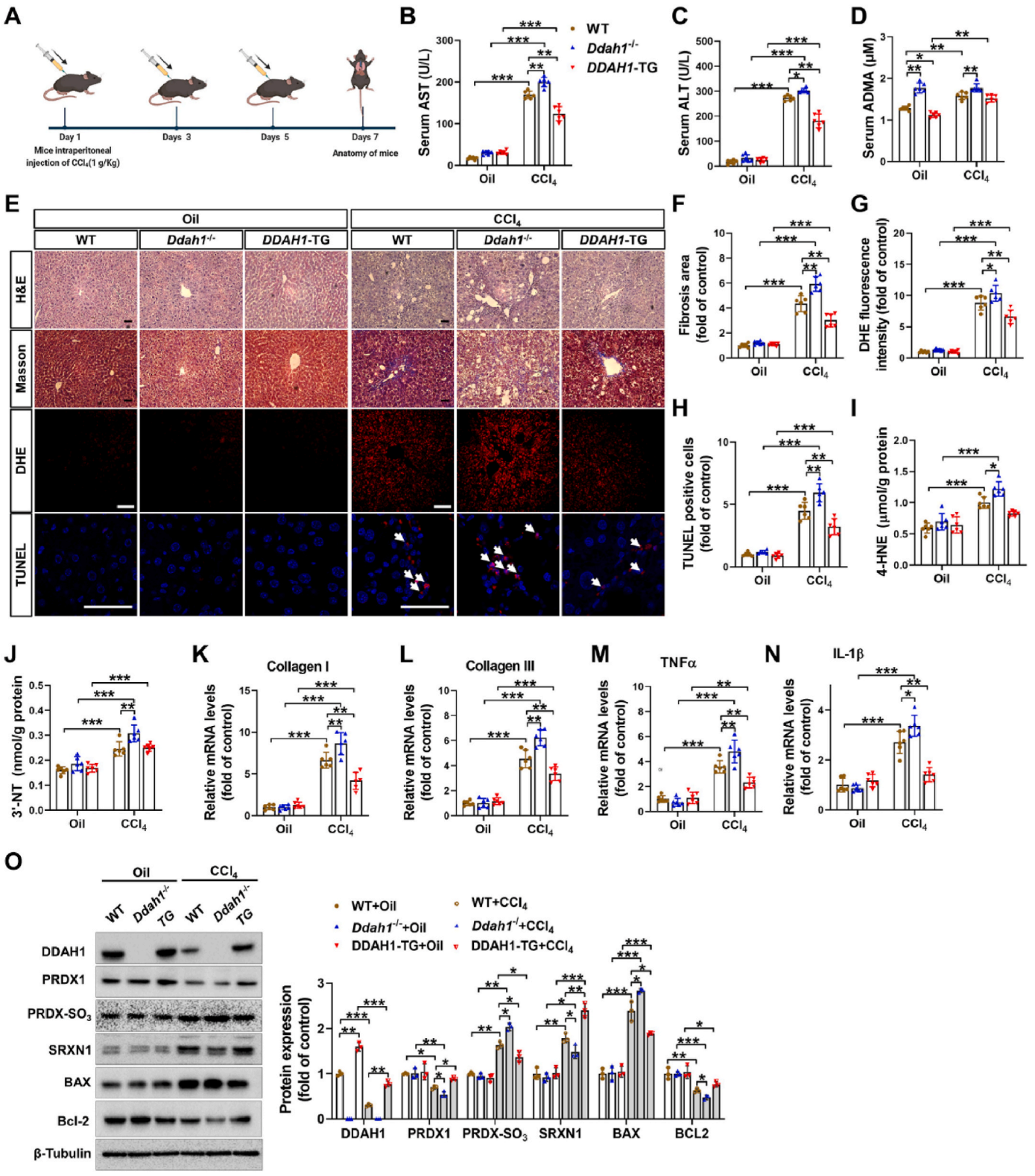

Fig. 5. DDAH1 alleviates CCl_4-induced hepatic fibrosis, oxidative stress, and apoptosis. (A) Schematic diagram illustrating the experimental process. After CCl_4 treatment, the serum levels of AST (B), ALT (C), and ADMA (D) were measured by commercial kits. (E) Representative liver sections from control and CCl_4-treated mice were stained with hematoxylin and eosin (H&E), Masson, DHE, and TUNEL assay kits. Scale bar = 50 μm. The relative fibrosis area (F), DHE fluorescence intensity (G), and number of TUNEL-positive cells (H) were quantified. The levels of 4-HNE (I) and 3′-NT (J) in the liver were measured in each group. (K–N) The mRNA levels of fibrotic and inflammatory genes were measured by qPCR. (O) Liver lysates were examined by western blotting. The values are expressed as the means ± SDs. In Fig. B–N, N = 6; in Fig. O, N = 3; *p < 0.05; **p < 0.01; ***p < 0.001; NS, not significant.

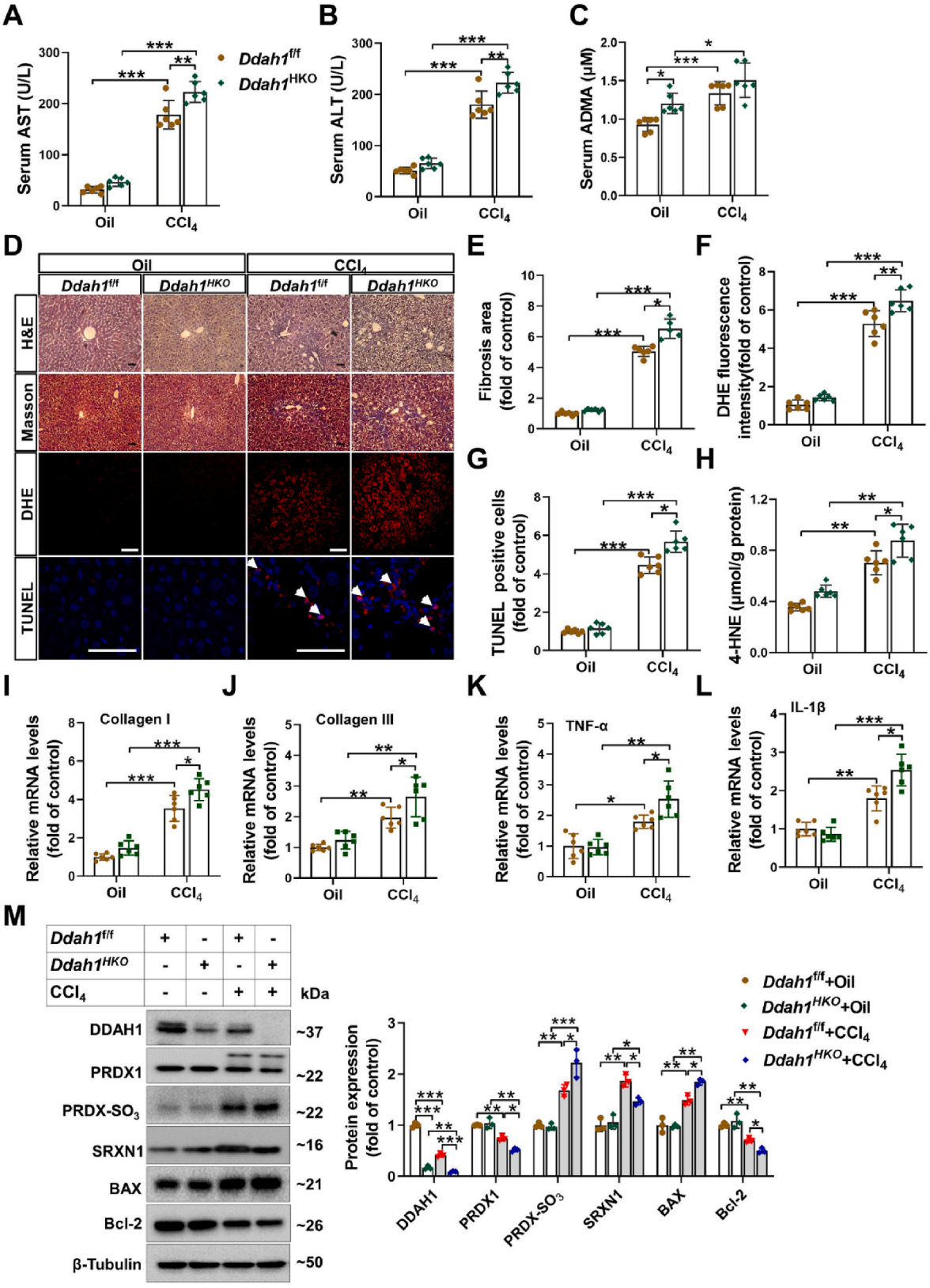

Fig. 6. Hepatic *Ddah1* deficiency aggravated liver dysfunction, oxidative stress, and apoptosis in mice treated with CCl_4. Male $Ddah1^{f/f}$ and $Ddah1^{HKO}$ mice were treated with CCl_4 by intraperitoneal injection and then their serum levels of AST (A), ALT (B), and ADMA (C) were measured. (D) Representative liver sections were stained with H&E, Masson, DHE, and TUNEL assay kits. Scale bar = 50 μm. The relative fibrosis area (E), DHE fluorescence intensity (F), and number of TUNEL-positive cells (G) were quantified. (H) Liver 4-HNE levels were measured in each group. (I–L) Liver mRNA levels of fibrotic and inflammatory genes were measured. (M) Liver lysates were examined by western blotting. The values are expressed as the means ± SDs. In Fig. A–L, N = 6; in Fig. M, N = 3; *p < 0.05; **p < 0.01; ***p < 0.001; NS, not significant.

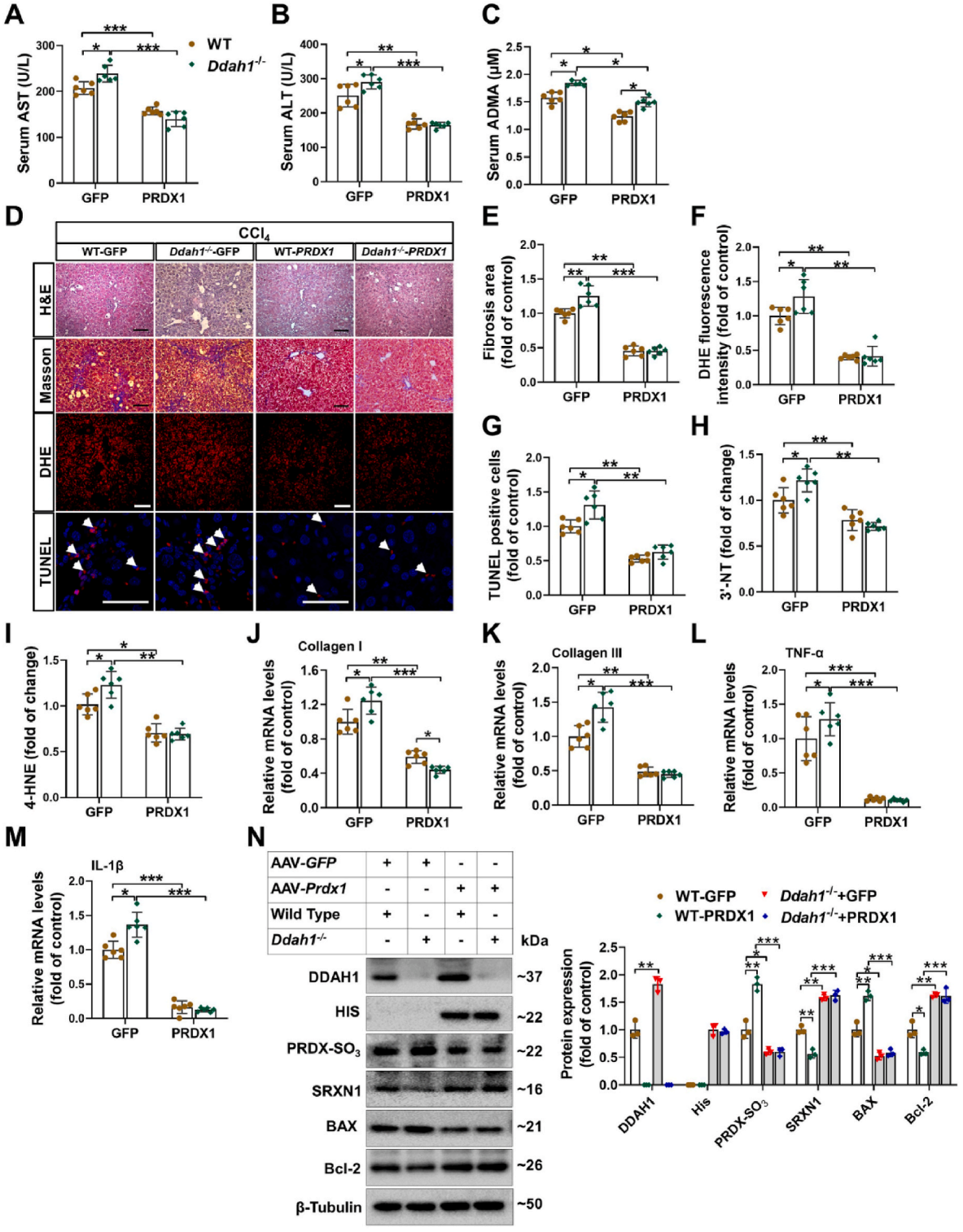

Fig. 7. PRDX1 overexpression improved CCl_4-induced liver injury, oxidative stress, and apoptosis. Male WT and *Ddah1*$^{-/-}$ mice were treated with AAV8-*GFP* or AAV8-*Prdx1* via tail vein injection. At 4 weeks after injection, the mice were treated with CCl_4 following the previous protocol. The mice were sacrificed, and the serum levels of AST (A), ALT (B), and ADMA (C) were measured. (D) Representative liver sections from each group were stained with H&E, Masson, DHE and TUNEL assay kits. Scale bar = 50 μm. The relative fibrosis area (E), DHE fluorescence intensity (F), and number of TUNEL-positive cells (G) were quantified. Liver 3′-NT (H) and 4-HNE (I) levels were determined in each group with respective ELISA kits. (J–M) The mRNA levels of fibrotic and inflammatory genes were measured by qPCR. (N) Liver lysates from each group were examined by western blotting. The values are expressed as the means ± SDs. In Fig. A–M, N = 6; in Fig. N, N = 3; *p < 0.05; **p < 0.01; ***p < 0.001.

with CCl_4 revealed that PRDX1 overexpression increased the expression of DDAH1, SRXN1, Bcl-2 and PRDX4 but decreased that of PRDX-SO_3 and Bax. Furthermore, the differences in the protein expression of PRDX-SO_3, SRXN1, Bcl-2, Bax and PRDX4 between the livers of WT and *Ddah1*$^{-/-}$ mice treated with CCl_4 were diminished after overexpression of PRDX1 (Fig. 7N, Fig. S6C).

4. Discussion

The present study revealed two major new findings. First, we demonstrated that DDAH1 interacted with PRDX1 and SRXN1 to maintain its expression and/or activity under oxidative stress conditions. Second, DDAH1 could maintain cell redox homeostasis by regulating the expression of PRDX1 and SRXN1 in response to oxidative stress.

There is evidence that DDAH1 is sensitive to oxidative stress. For example, H_2O_2 inactivates human DDAH1 in a time- and concentration-dependent manner [16]. DDAH1 activity or expression is also reduced by oxidative stress in different animal models, including those of diabetic nephropathy [29], polycystic ovary syndrome [30] and cirrhosis [31]. Herein, we showed that H_2O_2 decreased DDAH1 expression and dose-dependently increased intracellular ADMA levels in HepG2 cells. Treatment with CCl_4 also decreased hepatic DDAH1 expression and increased serum ADMA levels in mice. These results further confirmed that DDAH1 expression and activity were regulated by the cell redox state. Considering that oxidative stress plays an essential role in the pathogenesis of multiple diseases (e.g., congestive heart failure [32], NAFLD [33] and diabetes [4]), the elevated circulating ADMA levels in patients with these diseases could be the result of decreased tissue expression or activity of DDAH1.

Since DDAH1 is repressed by oxidative stress, it is reasonable to observe that antioxidant supplementation preserves DDAH1 activity and/or expression in different animal models [34,35]. However, it remains unclear whether there is any endogenous pathway that can protect DDAH1 against oxidation. PRDXs are a family of ancient and important antioxidant enzymes that eliminate H_2O_2, organic hydroperoxides and peroxynitrite [36]. Herein, we showed that DDAH1 interacted with PRDX1, PRDX4, and PRDX6 and that the interaction between DDAH1 and PRDX1 could be further enhanced by H_2O_2. Interestingly, PRDX1 negatively regulated intracellular ADMA levels without affecting DDAH1 expression in unstressed cells. Furthermore, PRDX1 overexpression attenuated, while PRDX1 knockdown exacerbated, the decreases in DDAH1 expression and the increases in intracellular ADMA levels in H_2O_2-treated HepG2 cells. PRDX1 overexpression also increased liver DDAH1 expression and decreased serum ADMA levels in mice treated with CCl_4. These findings suggest that DDAH1 may recruit PRDXs via protein–protein interactions to protect itself.

As a critical active site residue in human DDAH1, Cys^{274} may affect the susceptibility of DDAH1 to oxidation. H_2O_2-induced full inactivation of DDAH1 could be reversed by dithiothreitol, while L-lysine was found to increase the sensitivity of DDAH1 to H_2O_2 [16]. The present study showed that the C274A mutation impaired the interaction between DDAH1 and PRDX1, while the C275A and H173A mutations had no effect, suggesting that Cys^{274} is important for DDAH1 recruitment of PRDX1 and could be a potential protective target of PRDX1.

Cys^{52} and Cys^{173} in PRDX1 have been reported to be important for H_2O_2 catabolism and maintenance of cellular redox homeostasis [37,38]. Herein, we showed that the C52A and C173A mutations did not affect the DDAH1-PRDX1 interaction but led to a loss of the ability to protect against the H_2O_2-induced reduction in DDAH1 expression, suggesting that the antioxidant activity of PRDX1 is important for the maintenance of DDAH1 expression and activity. Upon extreme oxidative stress, aminoterminal Cys sulfenic acid (Cys-SOH) is overoxidized to sulfinic acid (Cys-SO_2H), leading to enzyme inactivation [39]. The levels of oxidized PRDXs could be reduced by the expression of SRXN1, an endogenous antioxidant enzyme that can effectively prevent cellular oxidative stress damage and apoptosis [40–42]. The present study showed that DDAH1 also interacted with SRXN1 and that this interaction was also enhanced by H_2O_2 but was not affected by the C274A mutation. Furthermore, SRXN1 overexpression attenuated, while SRXN1 knockdown aggravated, the overoxidation of PRDXs, decreases in DDAH1 and PRDX1 expression and increases in intracellular ADMA and ROS levels in H_2O_2-treated cells. Therefore, these results suggest that DDAH1 can also recruit SRXN1 to protect itself, which may be important for the preservation of DDAH1 under conditions of excessive oxidative stress.

The present study showed that DDAH1 overexpression attenuated, while DDAH1 knockdown exacerbated, cell death and ROS production in H_2O_2-treated cells. DDAH1 also exerted significant protective effects against CCl_4-induced hepatotoxicity. These results were consistent with our previous findings that DDAH1 has antioxidant effects on aged and diabetic kidneys [10], fatty livers [7], and $PM_{2.5}$-exposed lungs [11]. As ADMA accumulation can not only inhibit NO production but can also promote ROS production by uncoupling NOS [12], it is undisputed that the antioxidant effect of DDAH1 under stress conditions is related to ADMA degradation. However, we previously showed that the deletion of *Ddah1* in MEFs increased intracellular ROS levels, which could not be mimicked by the administration of exogenous ADMA [14]. Herein, we showed that the H173A mutation, which has been reported to inactivate DDAH1 [16], did not affect the antioxidant effect of DDAH1 in H_2O_2-treated HEK293 cells. Moreover, overexpression of DDAH1 did not affect the serum ADMA concentration but attenuated liver oxidative stress in mice treated with CCl_4. Similar results were observed in CCl_4-treated *Ddah1*$^{f/f}$ and *Ddah1*^{HKO} mice. Therefore, DDAH1 may also affect the cellular redox state through an ADMA-independent pathway.

The present study showed that DDAH1 overexpression attenuated PRDX1 downregulation in H_2O_2-treated cells and the livers of mice treated with CCl_4, while global or hepatocyte-specific deletion of *Ddah1* exacerbated CCl_4-induced PRDX1 downregulation. Furthermore, PRDX1 overexpression reduced the effect of *Ddah1* deficiency on CCl_4-induced hepatotoxicity. *Ddah1* deletion also attenuated the induction of SRXN1 and PRDX4 expression in the livers of CCl_4-treated mice. The regulatory effects of DDAH1 on antioxidant enzymes have also been observed in $PM_{2.5}$-exposed lungs [11] and in patients with cardiotoxin-induced muscle injury [9], acute myocardial infarction-induced heart failure [43] and diabetic nephropathy [10]. Notably, the underlying mechanism by which DDAH1 regulates antioxidant enzymes is complex and enzyme/cell/tissue dependent. For example, DDAH1 regulates SOD2 expression in MEFs via an NF-κB/miR-21-dependent pathway [14], while it regulates PRDX5 through an AMPK-dependent pathway in tubular epithelial cells [10]. DDAH1 deletion can also activate NRF2 by increasing intracellular ROS levels [44]. This mechanism could be responsible for the upregulation of PRDX1 and SRXN1 in HepG2 cells depleted of DDAH1. Herein, we showed that the DDAH1^{C274A} mutation could not preserve the expression of PRDX1 in H_2O_2-treated HEK293 cells. The C274A mutation at Cys^{274} also impaired the antioxidant effect of DDAH1 in H_2O_2-treated HEK293 and HepG2 cells. Therefore, DDAH1 is likely to partially regulate PRDX1 expression through protein–protein interactions, which are also important for the regulation of the cell redox state by DDAH1.

Although PRDX1 is primarily a H_2O_2 scavenging enzyme, its knockdown or overexpression significantly affected the DHE fluorescence intensity in H_2O_2-treated cells and CCl_4-challenged livers. The negative regulation on superoxide levels by PRDX1 has also been reported in bleomycin-treated BEAS-2B cells and lungs of mice [45]. It has been reported that H_2O_2 can increase superoxide levels and induce mitochondrial dysfunction in HUVEC cells [46]. H_2O_2 can also decrease SOD activity in HepG2 cells [47]. Moreover, PRDX1 knockout exacerbated the decreases in SOD activity and increases in H_2O_2 levels in the lungs of LPS-treated mice [48]. Therefore, it is possible that PRDX1 indirectly affects superoxide levels under stress conditions by

modulating H_2O_2 levels and SOD activity.

The present study has several limitations. First, DCFH-DA is not a H_2O_2 specific probe. Second, the peroxide scavenging activity of PRDX1 has not been measured in cells and livers. Therefore, our data could not provide the direct evidence to show that PRDX1 activity is directly altered by the interaction with DDAH1. Further evaluations of the PRDX1-DDAH1 interaction with purified proteins and advance technology are necessary in future studies.

In conclusion, our results provide the first direct evidence that DDAH1 can recruit PRDX1 and SRXN1 to maintain its activity/expression and redox homeostasis under oxidative stress conditions. Our results also suggest that targeting the DDAH1–PRDX1–SRXN1 interactions could be a novel therapeutic approach for liver diseases related to oxidative stress.

CRediT authorship contribution statement

Juntao Yuan: Writing – original draft, Methodology, Data curation, Conceptualization. **Zhuoran Yu:** Validation, Methodology, Investigation, Formal analysis, Data curation. **Ping Zhang:** Validation, Methodology, Data curation, Conceptualization. **Kai Luo:** Methodology, Investigation, Data curation. **Ying Xu:** Validation, Data curation. **Ting Lan:** Validation, Data curation. **Min Zhang:** Writing – review & editing, Supervision, Project administration, Methodology, Funding acquisition, Conceptualization. **Yingjie Chen:** Writing – review & editing, Supervision, Investigation, Funding acquisition, Data curation, Conceptualization. **Zhongbing Lu:** Writing – review & editing, Writing – original draft, Supervision, Project administration, Funding acquisition, Conceptualization.

Declaration of competing interest

The authors declare that they have no known competing financial interests or personal relationships that could have appeared to influence the work reported in this paper.

Data availability

Data will be made available on request.

Acknowledgments

This study was supported by grants from National Natural Science Foundation of China (82370275, 82070250 and 32200631), Beijing Hospitals Authority Clinical Medicine Development of special funding (ZLRK202308), Beijing Natural Science Foundation (5222029), China Postdoctoral Science Foundation (2022T150640) and the Fundamental Research Funds for the Central Universities.

Appendix A. Supplementary data

Supplementary data to this article can be found online at https://doi.org/10.1016/j.redox.2024.103080.

References

[1] Y. Tang, X. Zhou, T. Cao, E. Chen, Y. Li, W. Lei, Y. Hu, B. He, S. Liu, Endoplasmic Reticulum stress and oxidative stress in inflammatory diseases, DNA Cell Biol. 41 (11) (2022) 924–934.

[2] Z.Y. Liu, K. Song, B. Tu, L.C. Lin, H. Sun, Y. Zhou, R. Li, Y. Shi, J.J. Yang, Y. Zhang, J.Y. Zhao, H. Tao, Crosstalk between oxidative stress and epigenetic marks: new roles and therapeutic implications in cardiac fibrosis, Redox Biol. 65 (2023) 102820.

[3] A. Borrelli, P. Bonelli, F.M. Tuccillo, I.D. Goldfine, J.L. Evans, F.M. Buonaguro, A. Mancini, Role of gut microbiota and oxidative stress in the progression of non-alcoholic fatty liver disease to hepatocarcinoma: Current and innovative therapeutic approaches, Redox Biol. 15 (2018) 467–479.

[4] K. McKeegan, S.A. Mason, A.J. Trewin, M.A. Keske, G.D. Wadley, P.A. Della Gatta, M.G. Nikolaidis, L. Parker, Reactive oxygen species in exercise and insulin resistance: Working towards personalized antioxidant treatment, Redox Biol. 44 (2021) 102005.

[5] H.J. Forman, H. Zhang, Targeting oxidative stress in disease: promise and limitations of antioxidant therapy, Nat. Rev. Drug Discov. 20 (9) (2021) 689–709.

[6] X. Hu, D. Atzler, X. Xu, P. Zhang, H. Guo, Z. Lu, J. Fassett, E. Schwedhelm, R. H. Böger, R.J. Bache, Y. Chen, Dimethylarginine dimethylaminohydrolase-1 is the critical enzyme for degrading the cardiovascular risk factor asymmetrical dimethylarginine, Arterioscler. Thromb. Vasc. Biol. 31 (7) (2011) 1540–1546.

[7] X. Shen, K. Luo, J. Yuan, J. Gao, B. Cui, Z. Yu, Z. Lu, Hepatic DDAH1 mitigates hepatic steatosis and insulin resistance in obese mice: involvement of reduced S100A11 expression, Acta Pharm. Sin. B 13 (8) (2023) 3352–3364.

[8] T. Li, R. Feng, C. Zhao, Y. Wang, J. Wang, S. Liu, J. Cao, H. Wang, T. Wang, Y. Guo, Z. Lu, Dimethylarginine dimethylaminohydrolase 1 protects against high-Fat Diet-induced hepatic steatosis and insulin resistance in mice, Antioxidants Redox Signal. 26 (11) (2017) 598–609.

[9] F. Feng, B. Cui, L. Fang, T. Lan, K. Luo, X. Xu, Z. Lu, DDAH1 protects against cardiotoxin-induced muscle injury and regeneration, Antioxidants 12 (9) (2023).

[10] L. Shi, C. Zhao, H. Wang, T. Lei, S. Liu, J. Cao, Z. Lu, Dimethylarginine dimethylaminohydrolase 1 deficiency induces the epithelial to mesenchymal transition in renal proximal tubular epithelial cells and exacerbates kidney damage in aged and diabetic mice, Antioxidants Redox Signal. 27 (16) (2017) 1347–1360.

[11] J. Gao, T. Lei, H. Wang, K. Luo, Y. Wang, B. Cui, Z. Yu, X. Hu, F. Zhang, Y. Chen, W. Ding, Z. Lu, Dimethylarginine dimethylaminohydrolase 1 protects PM(2.5) exposure-induced lung injury in mice by repressing inflammation and oxidative stress, Part. Fibre Toxicol. 19 (1) (2022) 64.

[12] L.J. Druhan, S.P. Forbes, A.J. Pope, C.A. Chen, J.L. Zweier, A.J. Cardounel, Regulation of eNOS-derived superoxide by endogenous methylarginines, Biochemistry 47 (27) (2008) 7256–7263.

[13] O. Suda, M. Tsutsui, T. Morishita, H. Tasaki, S. Ueno, S. Nakata, T. Tsujimoto, Y. Toyohira, Y. Hayashida, Y. Sasaguri, Y. Ueta, Y. Nakashima, N. Yanagihara, Asymmetric dimethylarginine produces vascular lesions in endothelial nitric oxide synthase-deficient mice: involvement of renin-angiotensin system and oxidative stress, Arterioscler. Thromb. Vasc. Biol. 24 (9) (2004) 1682–1688.

[14] C. Zhao, T. Li, B. Han, W. Yue, L. Shi, H. Wang, Y. Guo, Z. Lu, DDAH1 deficiency promotes intracellular oxidative stress and cell apoptosis via a miR-21-dependent pathway in mouse embryonic fibroblasts, Free Radic. Biol. Med. 92 (2016) 50–60.

[15] V. Balasubramanian, G. Mehta, H. Jones, V. Sharma, N.A. Davies, R. Jalan, R. P. Mookerjee, Post-transcriptional regulation of hepatic DDAH1 with TNF blockade leads to improved eNOS function and reduced portal pressure in cirrhotic rats, Sci. Rep. 7 (1) (2017) 17900.

[16] L. Hong, W. Fast, Inhibition of human dimethylarginine dimethylaminohydrolase-1 by S-nitroso-L-homocysteine and hydrogen peroxide. Analysis, quantification, and implications for hyperhomocysteinemia, J. Biol. Chem. 282 (48) (2007) 34684–34692.

[17] J.C. Moon, G.M. Kim, E.K. Kim, H.N. Lee, B. Ha, S.Y. Lee, H.H. Jang, Reversal of 2-Cys peroxiredoxin oligomerization by sulfiredoxin, Biochem. Biophys. Res. Commun. 432 (2) (2013) 291–295.

[18] E.C. Ledgerwood, J.W. Marshall, J.F. Weijman, The role of peroxiredoxin 1 in redox sensing and transducing, Arch. Biochem. Biophys. 617 (2017) 60–67.

[19] A. Chatr-Aryamontri, B.J. Breitkreutz, S. Heinicke, L. Boucher, A. Winter, C. Stark, J. Nixon, L. Ramage, N. Kolas, L. O'Donnell, T. Reguly, A. Breitkreutz, A. Sellam, D. Chen, C. Chang, J. Rust, M. Livstone, R. Oughtred, K. Dolinski, M. Tyers, The BioGRID interaction database: 2013 update, Nucleic Acids Res. 41 (Database issue) (2013) D816–D823.

[20] A. Morinaka, Y. Funato, K. Uesugi, H. Miki, Oligomeric peroxiredoxin-I is an essential intermediate for p53 to activate MST1 kinase and apoptosis, Oncogene 30 (40) (2011) 4208–4218.

[21] R.A. Egler, E. Fernandes, K. Rothermund, S. Sereika, N. de Souza-Pinto, P. Jaruga, M. Dizdaroglu, E.V. Prochownik, Regulation of reactive oxygen species, DNA damage, and c-Myc function by peroxiredoxin 1, Oncogene 24 (54) (2005) 8038–8050.

[22] X. Shen, S.M. Ishaq, Q. Wang, J. Yuan, J. Gao, Z. Lu, DDAH1 protects against acetaminophen-induced liver hepatoxicity in mice, Antioxidants 11 (5) (2022).

[23] J. Yuan, Z. Yu, J. Gao, K. Luo, X. Shen, B. Cui, Z. Lu, Inhibition of GCN2 alleviates hepatic steatosis and oxidative stress in obese mice: involvement of NRF2 regulation, Redox Biol. 49 (2022) (2021) 102224.

[24] B. Kalyanaraman, V. Darley-Usmar, K.J. Davies, P.A. Dennery, H.J. Forman, M. B. Grisham, G.E. Mann, K. Moore, L.J. Roberts 2nd, H. Ischiropoulos, Measuring reactive oxygen and nitrogen species with fluorescent probes: challenges and limitations, Free Radic. Biol. Med. 52 (1) (2012) 1–6.

[25] J. Moffat, D.A. Grueneberg, X. Yang, S.Y. Kim, A.M. Kloepfer, G. Hinkle, B. Piqani, T.M. Eisenhaure, B. Luo, J.K. Grenier, A.E. Carpenter, S.Y. Foo, S.A. Stewart, B. R. Stockwell, N. Hacohen, W.C. Hahn, E.S. Lander, D.M. Sabatini, D.E. Root, A lentiviral RNAi library for human and mouse genes applied to an arrayed viral high-content screen, Cell 124 (6) (2006) 1283–1298.

[26] X. Xu, P. Zhang, D. Kwak, J. Fassett, W. Yue, D. Atzler, X. Hu, X. Liu, H. Wang, Z. Lu, H. Guo, E. Schwedhelm, R.H. Böger, P. Chen, Y. Chen, Cardiomyocyte dimethylarginine dimethylaminohydrolase-1 (DDAH1) plays an important role in attenuating ventricular hypertrophy and dysfunction, Basic Res. Cardiol. 112 (5) (2017) 55.

[27] S. Hirotsu, Y. Abe, K. Okada, N. Nagahara, H. Hori, T. Nishino, T. Hakoshima, Crystal structure of a multifunctional 2-Cys peroxiredoxin heme-binding protein 23 kDa/proliferation-associated gene product, Proc. Natl. Acad. Sci. U.S.A. 96 (22) (1999) 12333–12338.

[28] Z.A. Wood, E. Schröder, J. Robin Harris, L.B. Poole, Structure, mechanism and regulation of peroxiredoxins, Trends Biochem. Sci. 28 (1) (2003) 32–40.

[29] M.D. Wetzel, T. Gao, K. Stanley, T.K. Cooper, S.M. Morris Jr., A.S. Awad, Enhancing kidney DDAH-1 expression by adenovirus delivery reduces ADMA and ameliorates diabetic nephropathy, Am. J. Physiol. Ren. Physiol. 318 (2) (2020) F509–f517.
[30] T. Li, T. Zhang, H. Wang, Q. Zhang, H. Gao, R. Liu, C. Yin, The ADMA-DDAH1 axis in ovarian apoptosis of polycystic ovary syndrome, J. Steroid Biochem. Mol. Biol. 225 (2023) 106180.
[31] R.P. Mookerjee, G. Mehta, V. Balasubramaniyan, Z. Mohamed Fel, N. Davies, V. Sharma, Y. Iwakiri, R. Jalan, Hepatic dimethylarginine-dimethylaminohydrolase1 is reduced in cirrhosis and is a target for therapy in portal hypertension, J. Hepatol. 62 (2) (2015) 325–331.
[32] A. Daiber, O. Hahad, I. Andreadou, S. Steven, S. Daub, T. Münzel, Redox-related biomarkers in human cardiovascular disease - classical footprints and beyond, Redox Biol. 42 (2021) 101875.
[33] M.C. Podszun, J. Frank, Impact of vitamin E on redox biomarkers in non-alcoholic fatty liver disease, Redox Biol. 42 (2021) 101937.
[34] F. Nurkolis, N.A. Taslim, D. Subali, R. Kurniawan, H. Hardinsyah, W.B. Gunawan, R.J. Kusuma, V.M. Yusuf, A. Pramono, S. Kang, N. Mayulu, A.Y. Syauki, T.E. Tallei, A. Tsopmo, B. Kim, Dietary supplementation of caulerpa racemosa ameliorates cardiometabolic syndrome via regulation of PRMT-1/DDAH/ADMA pathway and gut microbiome in mice, Nutrients 15 (4) (2023).
[35] C.W. Lu, Y. Lin, Y.P. Lei, L. Wang, Z.M. He, Y. Xiong, Pyrrolidine dithiocarbamate ameliorates endothelial dysfunction in thoracic aorta of diabetic rats by preserving vascular DDAH activity, PLoS One 12 (7) (2017) e0179908.
[36] J. Bolduc, K. Koruza, T. Luo, J. Malo Pueyo, T.N. Vo, D. Ezeriņa, J. Messens, Peroxiredoxins wear many hats: factors that fashion their peroxide sensing personalities, Redox Biol. 42 (2021) 101959.
[37] B. Turner-Ivey, Y. Manevich, J. Schulte, E. Kistner-Griffin, A. Jezierska-Drutel, Y. Liu, C.A. Neumann, Role for Prdx1 as a specific sensor in redox-regulated senescence in breast cancer, Oncogene 32 (45) (2013) 5302–5314.
[38] T.N. Vo, J. Malo Pueyo, K. Wahni, D. Ezeriņa, J. Bolduc, J. Messens, Prdx1 interacts with ASK1 upon exposure to H(2)O(2) and independently of a scaffolding protein, Antioxidants 10 (7) (2021).
[39] A. Hall, P.A. Karplus, L.B. Poole, Typical 2-Cys peroxiredoxins–structures, mechanisms and functions, FEBS J. 276 (9) (2009) 2469–2477.
[40] J. Wu, Y. Chen, S. Yu, L. Li, X. Zhao, Q. Li, J. Zhao, Y. Zhao, Neuroprotective effects of sulfiredoxin-1 during cerebral ischemia/reperfusion oxidative stress injury in rats, Brain Res. Bull. 132 (2017) 99–108.
[41] K.C. Wu, J.J. Liu, C.D. Klaassen, Nrf2 activation prevents cadmium-induced acute liver injury, Toxicol. Appl. Pharmacol. 263 (1) (2012) 14–20.
[42] J. He, M. Ma, D. Li, K. Wang, Q. Wang, Q. Li, H. He, Y. Zhou, Q. Li, X. Hou, L. Yang, Sulfiredoxin-1 attenuates injury and inflammation in acute pancreatitis through the ROS/ER stress/Cathepsin B axis, Cell Death Dis. 12 (7) (2021) 626.
[43] L. Hou, J. Guo, F. Xu, X. Weng, W. Yue, J. Ge, Cardiomyocyte dimethylarginine dimethylaminohydrolase1 attenuates left-ventricular remodeling after acute myocardial infarction: involvement in oxidative stress and apoptosis, Basic Res. Cardiol. 113 (4) (2018) 28.
[44] H. Wang, Y. Guo, L. Liu, L. Guan, T. Wang, L. Zhang, Y. Wang, J. Cao, W. Ding, F. Zhang, Z. Lu, DDAH1 plays dual roles in PM2.5 induced cell death in A549 cells, Biochim. Biophys. Acta 1860 (12) (2016) 2793–2801.
[45] H.N. Sun, C.X. Ren, D.H. Lee, W.H. Wang, X.Y. Guo, Y.Y. Hao, X.M. Wang, H. N. Zhang, W.Q. Xiao, N. Li, J. Cong, Y.H. Han, T. Kwon, PRDX1 negatively regulates bleomycin-induced pulmonary fibrosis via inhibiting the epithelial-mesenchymal transition and lung fibroblast proliferation in vitro and in vivo, Cell. Mol. Biol. Lett. 28 (1) (2023) 48.
[46] H. Patel, J. Chen, M. Kavdia, Induced peroxidase and cytoprotective enzyme expressions support adaptation of HUVECs to sustain subsequent H2O2 exposure, Microvasc. Res. 103 (2016) 1–10.
[47] S. Sahoo, D. Rath, D.M. Kar, S. Pattanaik, Hepatoprotective potency of Litsea glutinosa (L.) C.B. Rob. leaf methanol extract on H(2)O(2)-induced toxicity in HepG2 cells, J. Ethnopharmacol. 304 (2023) 116076.
[48] W.P. Lv, M.X. Li, L. Wang, Peroxiredoxin 1 inhibits lipopolysaccharide-induced oxidative stress in lung tissue by regulating P38/JNK signaling pathway, Eur. Rev. Med. Pharmacol. Sci. 21 (8) (2017) 1876–1883.